ACOUSTICS 2012

Flaws detection using laser-ultrasound and mode conversion

F. Faese, F. Jenot, M. Ouaftouh and M. Duquennoy

IEMN-DOAE, Université de Valenciennes, Le Mont Houy, 59313 Valenciennes, France
frederic.faese@univ-valenciennes.fr

Industries such as the aeronautic industry or iron and steel industry are increasingly interested in laser ultrasonics, which is a cutting-edge technique used in non-destructive testing and evaluation. Compared to conventional methods such as piezoelectric transducers or EMATs, the main advantages of laser ultrasonics are a large bandwidth, its non-contact aspects and the ability to control high temperature and/or geometrically complex materials. Ultrasonic waves generation in an aluminium sample by a pulsed Nd:YAG laser, their detection by interferometry and their interaction with a slot are presented. Considering experimental results and finite element method simulation, the advantages of using a thermoelastic line generation as well as temporal and frequency effects of the slot on the surface acoustic waves will be explained. Associated with wave-conversion phenomena, these results lead to an original flaw detection and characterisation method.

1 Introduction

The physical processes governing acoustic waves generation by laser are well known and increasingly widespread in non destructive testing and evaluation applications [1,2]. Compared to conventional methods such as piezoelectric transducers or EMATs, laser ultrasonics has specific advantages: it is a non-contact method with a high spatial resolution and a large bandwidth. It allows high temperature and geometrically complex material testing.

Among the different kinds of lasers that have been used to generate ultrasonic waves, the most common one is the pulsed Nd:YAG laser [2]. In order to preserve the sample, the absorbed optical power density must be lower than the sample ablation threshold [3]. This threshold is typically for metals about 10 MW/cm². In that case, the ultrasonic waves are generated in the thermoelastic regime and, in metallic samples, the laser source essentially produces forces that are tangential to the sample surface.

Flaws detection and characterisation have been extensively studied [2,4]. The analysis techniques are mainly based on time-of-flight measurement, frequential analysis or diffraction signals study [5].

This paper describes the interaction between a thermoelastically generated Rayleigh wave and a slot machined in an aluminium block. By focusing on different waves, the slot is clearly highlighted and the effect of its orientation on the Rayleigh wave propagation is reported. A mode-converted wave related to the slot is also investigated. Both experimental results and finite element calculations show that this wave could lead to a complete slot characterisation: width, depth and geometry.

2 Laser-ultrasonics excitation of Rayleigh waves

The only surface acoustic waves able to propagate on a semi-infinite isotropic solid placed in vacuum are the Rayleigh waves.

Let v_S and v_L be the shear and the longitudinal wave velocity in the material respectively. The real solution of the following equation corresponds to the Rayleigh wave velocity v_R:

$$\left(\frac{v}{v_S}\right)^6 - 8\left(\frac{v}{v_S}\right)^4 + 8\left(3 - 2\left(\frac{v_S}{v_L}\right)^2\right)\left(\frac{v}{v_S}\right)^2 - 16\left(1 - \left(\frac{v_S}{v_L}\right)^2\right) = 0 \quad (1)$$

This velocity is slightly lower than the shear wave velocity in the material. An approximate solution is given by the following equation [6]:

$$v_R \approx v_S \frac{0{,}87 + 1{,}12\eta}{1+\eta} \quad (2)$$

where η is the Poisson's ratio.

When the Rayleigh waves are generated by a thermoelastic line source, their energy is concentrated on a specific direction perpendicular to the line source and passing through its middle [7]. The directivity diagrams for two line sources having different lengths are given in Figure 1.

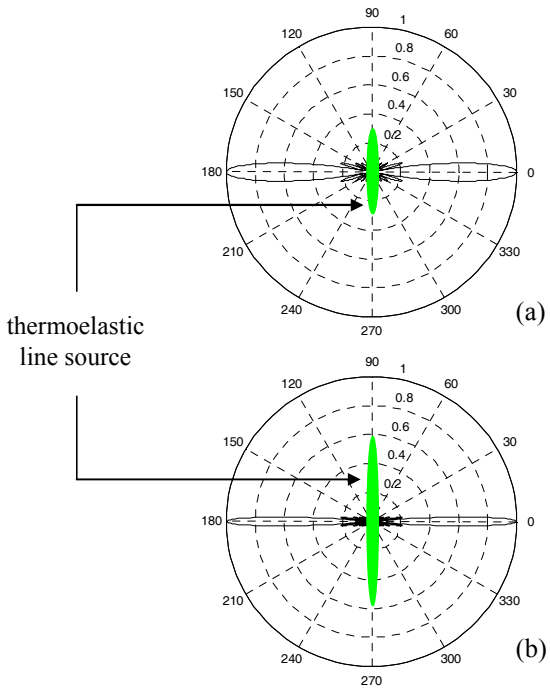

Figure 1: Rayleigh waves directivity diagrams in aluminium at an acoustic frequency of 3 MHz with an infinitely thin thermoelastic line source 5 mm (a) and 10 mm (b) long

3 Experimental set-up

The set-up used to generate and detect the surface acoustic waves is represented in Figure 2 [8]. A Q-switched Nd:YAG laser emitting 10 ns pulses with a wavelength of 532 nm is focalised by a cylindrical lens. The line source is approximately 6 mm long and 0.2 mm wide. The energy per pulse is about 5 mJ on the sample surface, which allows to work in the thermoelastic mode.

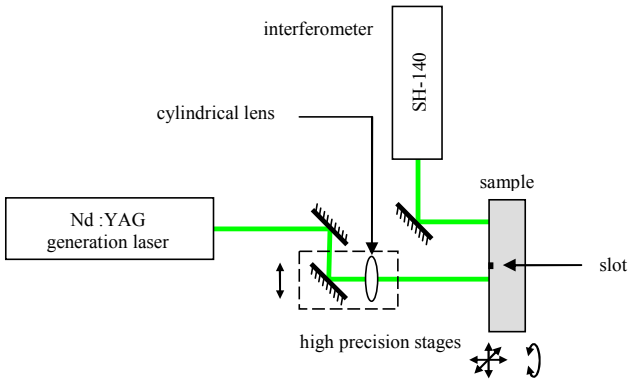

Figure 2: experimental set-up used to generate and detect surface acoustic waves

The normal surface displacement is measured by a Mach-Zehnder interferometer having a wide bandwidth (between 200 kHz and 45 MHz) and emitting a continuous 532 nm of wavelength 100 mW beam. The received signals are sampled and averaged by a digital oscilloscope before recording. In order to improve the signal to noise ratio, each record is obtained by averaging 80 laser shots.

The sample is a 20 mm thick aluminium block. A 300 µm wide and 300 µm deep slot has been machined in the middle of the sample.

As shown in Figure 3, the normal displacement is measured by interferometry when the acoustic wave is either transmitted or reflected by the slot. θ corresponds to the Rayleigh wave incident angle on the slot.

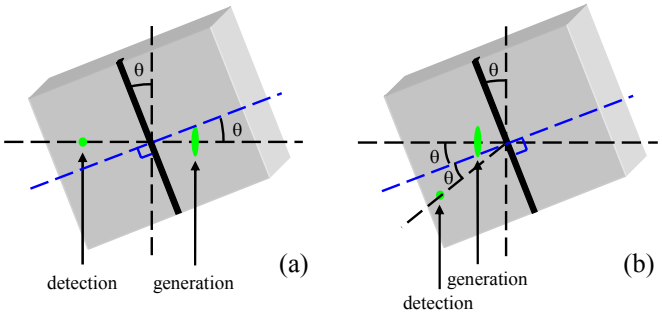

Figure 3: experimental set-ups associated with transmission (a) and reflection (b) measurements

4 Experimental results and discussions

4.1 Influence of the incidence angle

The Rayleigh wave transmitted by the slot was recorded for θ in the range of 0° to 65°. The signals and their spectra are presented in Figure 4 for the angles θ = 0° and θ = 60°.

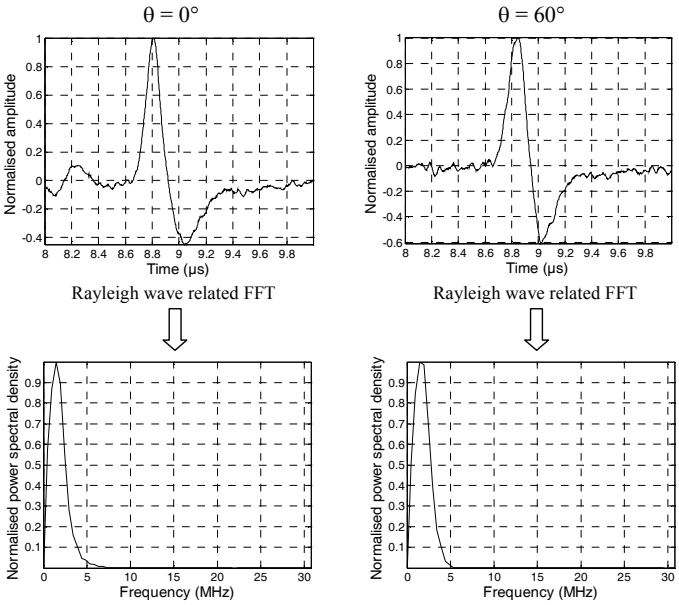

Figure 4: normal displacement after transmission by the slot and associated spectra (θ = 0° and θ = 60°)

By varying θ, no significant effect can be observed on the previous signals.

The Rayleigh wave reflected by the slot and its related spectrum were recorded for θ in the range of 0° to 18°. The corresponding signals are shown in Figure 5 for θ = 0° and θ = 15°.

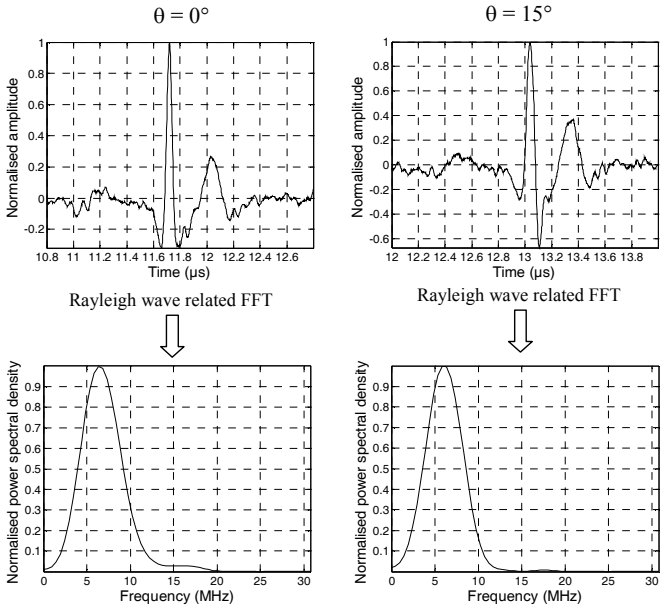

Figure 5: normal displacement after reflection by the slot and associated spectra (θ = 0° and θ = 15°)

The highest amplitude of the reflected signal is measured when the detection point is placed on a direction whose angle compared to the direction of the incident wave equals 2θ, hence verifying the Snell-Descartes law. Some slight changes on the detected signals are observed but there is no clear correlation between these changes and θ. However, knowing the generation and detection positions, the time of flight of the reflected wave allows to obtain some information on the position and the orientation of the slot.

The spectra related to the reflected waves have higher frequencies than the spectra related to the transmitted waves. The slot can be considered as a low-pass filter in transmission and a high-pass filter in reflection. This is in good agreement with other literature results [9,10].

4.2 Conversion phenomena

From now on, θ is set to 0°. Some of the first observed signals are presented below.

Let d_{GS}, d_{SD} and d_{GD} be respectively the distance between generation and the slot, between the slot and detection and between generation and detection.

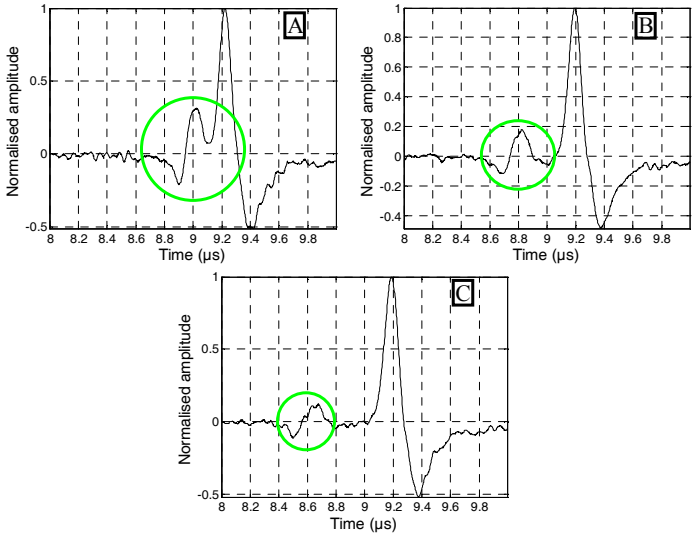

Figure 6: transmitted signals when d_{GD} = 27 mm and d_{GS} = 2 mm (A), 3 mm (B) and 4 mm (C)

In Figure 6, another wave called "secondary wave" clearly appears before the Rayleigh wave. The amplitude of this wave is sensitive to the distance d_{GS}.

In Figure 7, the distance d_{GS} is kept constant while the distance d_{SD} is increased.

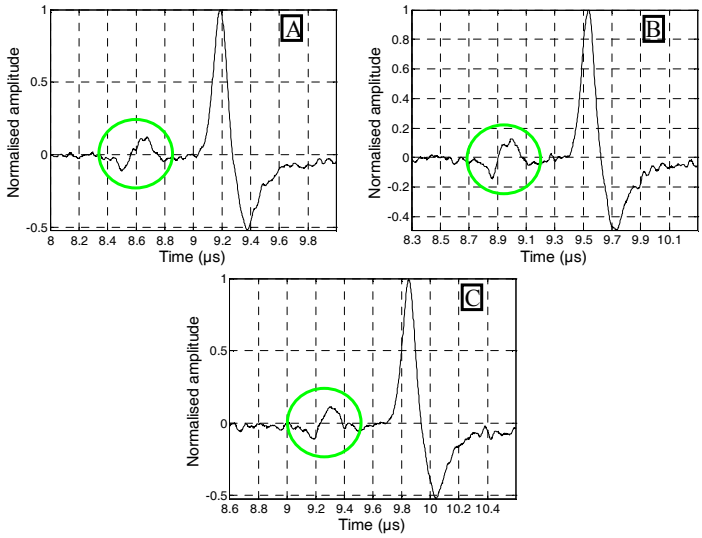

Figure 7: transmitted signals when d_{GS} = 4 mm and d_{SD} = 23 mm (A), 24 mm (B) and 25 mm (C)

Using the "secondary wave" time of flight (zero crossing method) and the corresponding propagation distance related to d_{SD}, a linear regression gives the velocity of this wave after the slot. It was found 2 980 m.s^{-1}.

In Figure 8, the distance d_{SD} is kept constant while the distance d_{GS} is increased.

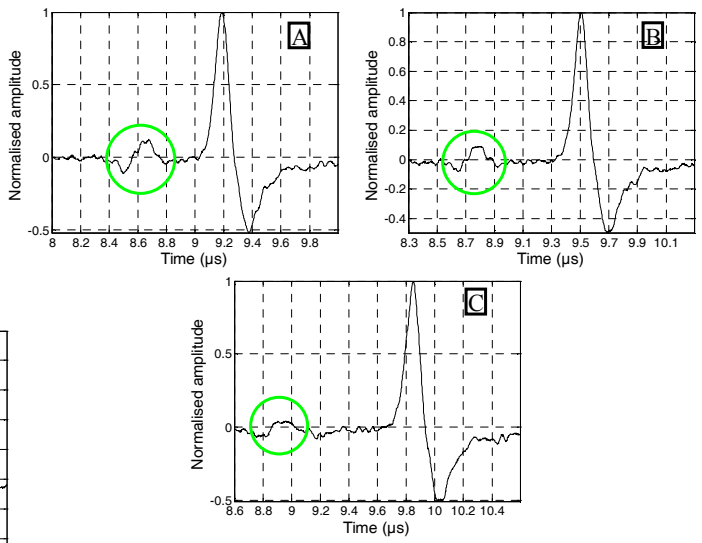

Figure 8: transmitted signals when d_{SD} = 23 mm and d_{GS} = 4 mm (A), 5 mm (B) and 6 mm (C)

Considering the distance d_{GS} and the different times of flight, the "secondary wave" velocity before the slot is estimated to 6 710 m.s^{-1}.

The "secondary wave" velocity before the slot is close to the longitudinal wave velocity in aluminium ($v_L \approx 6\,360$ m.s^{-1}) whereas after the slot it is close to the Rayleigh wave velocity in this material ($v_R \approx 2\,920$ m.s^{-1}).

By neglecting the slot dimensions compared to the propagation distance, let us assume the "secondary wave" travels the distance d_{GS} with a velocity v_L and the distance d_{SD} with a velocity v_R. Let t_S and t_R be respectively the "secondary wave" and the Rayleigh wave times of flight and Δt the difference $t_R - t_S$. The relation between these values is:

$$t_S = \frac{d_{GS}}{v_L} + \frac{d_{SD}}{v_R} \Leftrightarrow d_{GS} = \left(\frac{v_L . v_R}{v_L - v_R} \right) . \Delta t \qquad (3)$$

Thus, the time of flight difference Δt between the Rayleigh wave and the "secondary wave" would be directly proportional to the distance between the generation and the slot.

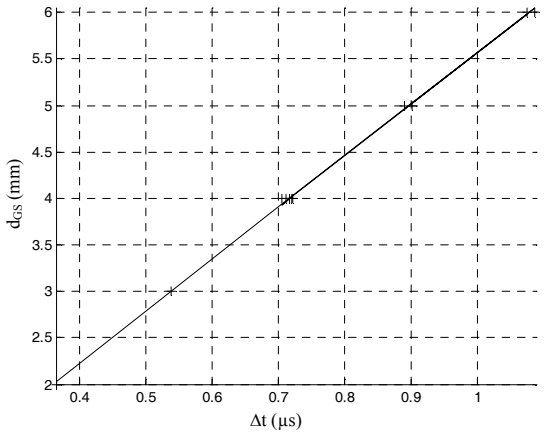

Figure 9: distance between the generation and the slot (d_{GS}) as a function of the time of flight difference between the Rayleigh wave and the "secondary wave" (Δt)

Figure 9 shows the linear regression obtained using the experimental results, which gives $(d_{GS}/\Delta t)_{exp} \approx 5\ 560$ m.s^{-1}. The experimental values are in good agreement with the theoretical ones $(d_{GS}/\Delta t)_{th} \approx 5\ 400$ m.s^{-1}.

5 Finite element method results

Figure 10 clearly shows the acoustic waves generated after a laser shot on a semi-infinite aluminium sample placed in vacuum. The longitudinal and shear waves as well as the head and Rayleigh waves are clearly predicted. Depending on the slot, the « secondary wave » is also observed.

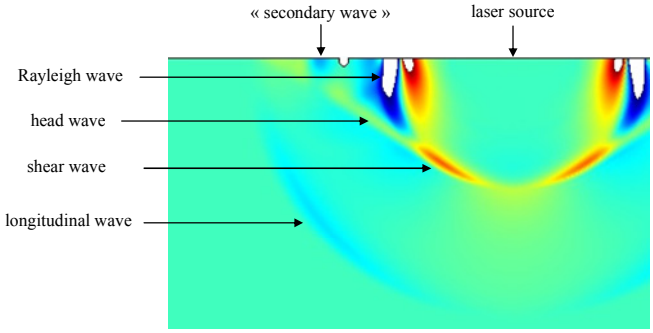

Figure 10: calculated normal displacement in aluminium (0,5 µs after the laser shot)

Figure 11 represents the normal displacement as a function of time for d_{GS} = 2 mm and d_{SD} = 6 mm.

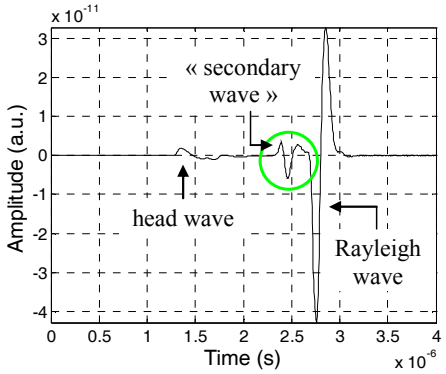

Figure 11: calculated normal displacement as a function of time for d_{GS} = 2 mm, d_{SD} = 6 mm

The calculated displacement is in good agreement with the previous measurements.

The simulation also confirms that the "secondary wave" is composed of the head wave before the slot which is then converted by this flaw into a Rayleigh wave.

6 Conclusion and perspectives

The slot orientation influence on the transmitted and reflected surface acoustic waves has been studied. Slight changes, with time and frequency, were observed but there was no evidence for a correlation between these changes and the slot orientation. However, the measures clearly showed that, in the frequency domain, the slot acted as a low-pass filter in transmission and a high-pass filter in reflection. Moreover, as the reflected wave ideally followed the Snell-Descartes law, this wave was able to give some information on the slot position and orientation.

The experimental results also revealed a transmitted wave that was smaller in amplitude and preceding the Rayleigh wave. This wave propagated before the slot with the longitudinal wave velocity and after the slot with the Rayleigh wave velocity. As it was assumed after these experimental results, the finite element method calculations tended to show that this wave came from the mode conversion of the head wave in a secondary Rayleigh wave at the slot. Further analysis on this "secondary wave" could allow a more detailed slot characterisation, especially regarding its geometrical features.

Acknowledgments

The authors thank the help obtained from the ANR for its contribution in ECO CND project through its support in the "production durable et technologies de l'environnement ECOTECH" program.

References

[1] R.M. White, Generation of Elastic Waves by Transient Surface Heating, Journal of Applied Physics, Vol. 34-12, 1963, pp. 3559-3567

[2] C.B. Scruby and L.E. Drain, Laser Ultrasonics, Adam Hilger, Bristol, 1990

[3] J.F. Ready, Effect of high power radiation, Academic Press New York, 1971

[4] P.A. Doyle and C.M. Scala, Crack depth measurement by ultrasonics: a review, Ultrasonics, 1978, pp. 164-170

[5] J.P. Charlesworth and J.A.G. Temple, Engineering Applications of Ultrasonic Time of Flight Diffraction, Wiley, New York, 1989

[6] I.A. Viktorov, Rayleigh and Lamb waves - physical theory and applications, Ultrasonic Technology, Plenum Press, New York, 1967

[7] A.M. Aindow et al., Laser-generation of directional surface acoustic wave pulses in metals, Optics Communications, Vol. 42-2, 1982, pp. 116-120

[8] F. Jenot et al., Interferometric detection of acoustic waves at air-solid interface applications to non-destructive testing, Journal of Applied Physics, 97 094905, 2005

[9] G. Hévin, et al., Characterisation of surface cracks with Rayleigh waves: a numerical model, NDT&E International, Vol. 31-4, 1998, pp. 289-297

[10] B. Masserey and E. Mazza, Ultrasonic sizing of short surface cracks, Ultrasonics, Vol. 46, 2007, pp. 195-204